A SOCP Relaxation for Cycle Constraints in the Optimal Power Flow Problem

Arash Farokhi Soofi, *Student Member, IEEE* and Saeed D. Manshadi, *Member, IEEE*, Guangyi Liu, *Senior Member, IEEE*, Renchang Dai, *Senior Member, IEEE*

***Abstract*—This paper presented a convex relaxation approach for the optimal power flow problem. The proposed approach leveraged the second-order cone programming (SOCP) relaxation to tackle the non-convexity within the feasible region of the power flow problem. Recovering an optimal solution that is feasible for the original non-convex problem is challenging for networks with cycles. The main challenge is the lack of convex constraints to present the voltage angles within a cycle. This paper aims to fill this gap by presenting a convex constraint enforcing the sum of voltage angles over a cycle to be zero. To this end, the higher-order moment relaxation matrix associated with each maximal clique of the network is formed. The elements of this matrix are utilized to form a convex constraint enforcing the voltage angle summation over each cycle. To keep the computation burden of leveraging the higher-order moment relaxation low, a set of second-order cone constraints are applied to relate the elements of the higher-order moment relaxation matrix. The case study presented the merit of this work by comparing the solution procured by the introduced approach with other relaxation schemes.**

***Index Terms*—optimal power flow, convex relaxation, angle recovery, second-order cone programming, nonlinear programming.**

NOMENCLATURE

Sets

$\mathcal{G}$	Set of generation units
$\mathcal{G}_i$	Set of all generation units connected to bus i
$\mathcal{L}$	Set of distribution lines
$\mathcal{N}$	Set of all buses
δ_i	Set of all buses connected to bus i

Variables

V_i	Voltage phasor of bus i
e_i	Real part of voltage phasor of bus i
f_i	Imaginary part of voltage phasor of bus i
p_g, q_g	Real and reactive power generation output of unit g
p_i^d, q_i^d	Real and reactive power demand at bus i
θ_i	Voltage angle of bus i
c, s	Lifting variable terms for SOCP relaxation
p_{ij}, q_{ij}	Real and reactive power flow from bus i to bus j
θ_{ij}	The difference between voltage phase angle of bus i and bus j
$\gamma(.)$	Lifting operator for the moment relaxation matrix

Parameters

C_g	Generation cost function of generator g
$G_{(.)}$	Elements of the conductance matrix
$B_{(.)}$	Elements of the susceptance matrix
V_i^{min}	Minimum voltage magnitude at bus i
V_i^{max}	Maximum voltage magnitude at bus i
p_g^{min}, p_g^{max}	Real power generation limits of unit g
q_g^{min}, q_g^{max}	Reactive power generation limits of unit g
S_{ij}^{max}	Maximum apparent power of the branch connecting buses i and j

Arash Farokhi Soofi and S. D. Manshadi are with San Diego State University, San Diego, CA, 92182 USA. e-mail: afarokhisoofi@sdsu.edu; smanshadi@sdsu.edu. G. Liu and R. Dai are with the Global Energy Interconnection Research Institute North America, San Jose, CA 95134 USA (e-mail: guangyi.liu@geiri.net; renchang.dai@geiri.net).

I. INTRODUCTION

OPTIMAL power flow (OPF) is the underlying problem for many power system operational planning problems that its AC form is introduced in [1]. ACOPF is a non-convex optimization problem that is hard to solve in polynomial time [2], [3]. The traditional solution methods (e.g. interior-point and gradient-based) may converge to local optimal solutions [4]. Moreover, due to the non-convexity of the problem, it may fail to converge for some systems depending on the initial guess [5]. To remedy this issue, a set of convex relaxation approaches are presented to find the optimal solution or at least its lower bound. Semi-definite programming (SDP) [6], second-order cone programming (SOCP) [7], and quadratic convex (QC) [8] relaxations are among those relaxation approaches. Although these convex relaxation approaches can provide a polynomial-time algorithm to solve the problem, they are suffering from two major issues. The first issue is that the solution to the relaxed problem might not be feasible for the original non-convex problem [9], [10]. To improve the exactness of these convex relaxation approaches, bound tightening methods are presented in the literature. Several tightening methods are presented in [11] for QC relaxation problem formulation. The McCormick envelops are leveraged in [12] to strengthen the SOCP relaxation problem. Another route to overcome the tightness issue is to employ moment-based approaches which guarantee that when the order of the moment relaxation goes to infinity, the relaxation is exact [13], [14]. However, the computation burden of employing higher orders of moment relaxation is very large that makes it an impractical problem to solve. This raises the second drawback of convex relaxation approaches which is the lack of reliable and efficient solvers specifically for large-scale SDP problems. Employing the sparse form of the moment relaxation matrix could mitigate the computation burden. According to the PSD matrix completion theorem [15], a matrix is PSD if and only if each submatrix, formed based on the maximal cliques of

the associated graph of the network, is also PSD. Although leveraging sparsity leads to a decrease in the computation burden of higher-order moment relaxation approaches for the medium-size network (e.g. up to 300 bus), it is still hardly practical for larger size networks [16]. Sparsity enables the solution of the first-order moment relaxation for systems with thousands of buses [17] and the second-order moment relaxation for systems with approximately forty buses [18]. One remedy to the issue is presented in [19], the first-order relaxation is formulated with SDP constraints and the higher-order relaxations are presented by SOCP constraints. Another approach to overcome this challenge is to employ cycle-based SDP relaxation methods as suggested in [20] which led to a reduction in the computation complexity of SDP relaxation problems compared to clique-based approaches. The focus of this paper is to leverage cycle constraint to present a convex relaxation approach with an enhanced tightness and moderate computation burden.

On one hand, the ACOPF solution procured by SDP relaxation for meshed networks is tighter than the one procured by SOCP and QC relaxations, but for the radial networks, SOCP and SDP relaxation methods are equivalent [21], [22]. On the other hand, solving the ACOPF problem using SOCP and QC relaxations is more efficient than using SDP relaxation. There is a research trend to present a set of valid constraints to the SOCP and QC relaxations of the ACOPF problem to enhance its tightness and reach a tightness comparable to SDP relaxation. Angle recovery is the main challenge for the SOCP-based ACOPF problem. A set of strong SOCP and SDP relaxations are presented in [23], [24], and [25] to enforce the angle over a cycles within power network. In [26], the semi-definiteness constraint is relaxed by the second-order cone constraint for each principal minor. The SOCP relaxation is then further tightened by polynomial cuts. The procured problem is nonlinear but convex and the procured solution is a globally optimal solution with a much lighter computation burden compared to utilization of SDP solvers. However, the procured relaxation is at most as tight as the SDP relaxation and could still render solutions with a rank higher than one. In [27], it is discussed that the problem reformulation can uncover a hidden rank-1 solution. In [28], it is shown that rank constraints can be reformulated by both principal and non-principal of 2×2 minors of the Hermitian matrix associated with the lifting variables of the ACOPF problem discussed in [29]. It is argued that it is equivalent to enforcing cycle constraints of SOCP relaxation of the ACOPF problem. They proposed strong cutting planes, convex envelopes, and bound tightening techniques to strengthen the resulting SOCP relaxations. The approach presented here aims to explore another path to tighten the SOCP relaxation by introducing a set of valid cuts enforcing the cycle constraints.

The main contributions of this paper are listed as follows.

- A convex relaxation approach is presented to enforce non-convex cycle constraints which are not presented in the SOCP relaxation of the AC-OPF problem. It is shown that when the presented relaxation approach is employed, the summation of voltage angle differences over the cycles of a network is much smaller than that of employing the SOCP relaxation method.
- Leveraging the chordal extension of the graph associated with the network to build up cycles with 3 vertices that are suitable for formulating the cycle constraints using the terms within the second order-moment relaxation matrix.
- A second-order cone relaxation is presented for the second-order moment relaxation matrix which mitigate the computation burden of utilizing the lifting terms of the second-order moment relaxation matrix in the presented cycle constraint relaxation method.

II. Problem Formulation

The problem formulation for the ACOPF problem in rectangular form is presented in (1). The total cost of generation is minimized as shown in (1a). The real and reactive power flow sending from bus i to bus j are given in (1b) and (1c), respectively. The nodal balance equations for the real and reactive power at each bus are shown in (1d) and (1e), respectively. The upper limit and lower limit of voltage magnitude at each bus are given in (1f), where the voltage limits are presented in their square form.. The physical limits of real and reactive power generation for each generation unit are presented in (1g) and (1h), respectively. The thermal limits of the apparent power sending from bus i to bus j is shown in (1i).

$$\min \sum_{g \in \mathcal{G}} C_g(p_g) \tag{1a}$$

s.t.

$$\begin{cases} p_{ij} = -G_{ij}(e_i^2 + f_i^2) + \\ G_{ij}(e_i e_j + f_i f_j) - B_{ij}(e_i f_j - e_j f_i) \end{cases} \quad \forall (i,j) \in \mathcal{L} \tag{1b}$$

$$\begin{cases} q_{ij} = B_{ij}(e_i^2 + f_i^2) - \\ B_{ij}(e_i e_j + f_i f_j) - G_{ij}(e_i f_j - e_j f_i) \end{cases} \quad \forall (i,j) \in \mathcal{L} \tag{1c}$$

$$\begin{cases} \sum_{g \in \mathcal{G}_i} p_g - p_i^d = \\ (G_{ii} + \sum_{j \in \delta_i} G_{ij})(e_i^2 + f_i^2) + \sum_{j \in \delta_i} p_{ij} \end{cases} \quad \forall i \in \mathcal{N} \tag{1d}$$

$$\begin{cases} \sum_{g \in \mathcal{G}_i} q_g - q_i^d = \\ -(B_{ii} + \sum_{j \in \delta_i} B_{ij})(e_i^2 + f_i^2) + \sum_{j \in \delta_i} q_{ij} \end{cases} \quad \forall i \in \mathcal{N} \tag{1e}$$

$$(V_i^{min})^2 \leq e_i^2 + f_i^2 \leq (V_i^{max})^2 \quad \forall i \in \mathcal{N} \tag{1f}$$

$$p_g^{min} \leq p_g \leq p_g^{max} \quad \forall g \in \mathcal{G} \tag{1g}$$

$$q_g^{min} \leq q_g \leq q_g^{max} \quad \forall g \in \mathcal{G} \tag{1h}$$

$$0 \leq \sqrt{p_{ij}^2 + q_{ij}^2} \leq S_{ij}^{max} \quad \forall (i,j) \in \mathcal{L} \tag{1i}$$

The problem formulation presented in (1) is a non-convex problem. Solving this problem with iterative approaches may fail to find an optimal solution. A solution method that aims to leverage second-order cone programming relaxation with an enhanced tightness by leveraging the cycle constraints is presented in the next section of this paper.

III. Solution Methodology

A. Overview

To find the solution to the problem presented in (1), a relaxation scheme is presented in this section. The problem that is presented in (1) is an NP-hard problem. Nonlinear solution methodologies cannot guarantee to find a solution in polynomial time. First, the problem formulation is reformulated using the SOCP relaxation technique. Although such relaxation presents a computationally light solution method, it presents a

zero relaxation gap only for radial networks. To obtain a zero-gap solution for mesh networks, the voltage angles must be precisely recovered. Thus, the next subsection presented a set of cycle constraints to enforce proper voltage angles across the network. However, the procured terms exhibit bilinear terms of the SOCP relaxed terms which are further relaxed using the second-order moment relaxation matrix associated with the chordal extension of the network. Finally, in the next subsection, a SOCP relaxation is presented for the procured moment relaxation problem to facilitate rewriting the original non-convex OPF problem formulated in (1) in a new convex relaxation form denoted as cycle constraint relaxation. The following subsections discuss the measure for the tightness of the presented relaxation as well as an angle recovery scheme.

B. The Primary SOCP Relaxation

The rectangular formulation of the ACOPF problem presented in (1) is a non-convex quadratic optimization problem. The source of non-convexity is the bi-linear terms in branch flow equality constraints given in (1b) and (1c). A set of lifting variables is introduced in (2) to relax the problem presented in (1).

$$c_{ii} := e_i^2 + f_i^2 = V_i^* V_i \tag{2a}$$
$$c_{ij} := e_i e_j + f_i f_j = \mathbf{Re}\{V_i^* V_j\} \tag{2b}$$
$$s_{ij} := e_i f_j - f_i e_j = \mathbf{Im}\{V_i^* V_j\} \tag{2c}$$

For any given angle difference of pair of buses, the trigonometric relationship given in (3a) holds. Once the equation given in (3a) is multiplied by $(|V_i|\,|V_j|)^2$, it is presented as given in (3b). This equation is further presented in phasor form as given in (3c). Applying the lifting terms introduced in (2), the equation presented in (3c) is reformulated in the form presented in (3d).

$$\cos\theta_{ij}{}^2 + \sin\theta_{ij}{}^2 = 1 \tag{3a}$$
$$(|V_i|\,|V_j|\cos\theta_{ij})^2 + (|V_i|\,|V_j|\sin\theta_{ij})^2 = |V_i|^2\,|V_j|^2 \tag{3b}$$
$$(\mathbf{Re}\{V_i^* V_j\})^2 + (\mathbf{Im}\{V_i^* V_j\})^2 = (V_i^* V_i)(V_j^* V_j) \tag{3c}$$
$$c_{ij}^2 + s_{ij}^2 = c_{ii} c_{jj} \tag{3d}$$

The defined lifting terms in (2) are leveraged to reformulate the original ACOPF problem given in (1) to the form presented in (4). This relaxation is referred to as the SOCP relaxation of the ACOPF problem as discussed in [23] and [29]. Here, the objective function is the same as the one in the original non-convex problem. The non-convex equality constraints presented in (1b)-(1c) are represented in a conic relaxed form as represented (4b)-(4c) using the lifting terms introduced in (2). The voltage limits are presented in terms of the lifting terms as given in (4f). The relationships between the lifting terms of each pair of buses are given in (4g). The second-order cone constraint given in (4h) presents the second-order cone relaxation of the relationship between the lifting terms given in (3d). The rest of the constraints in (4) are the same as those presented in (1).

$$\min \sum_{g\in\mathcal{G}} C_g(p_g) \tag{4a}$$
s.t.
$$p_{ij} = -G_{ij}c_{ii} + G_{ij}c_{ij} - B_{ij}s_{ij} \qquad \forall (i,j)\in\mathcal{L} \tag{4b}$$
$$q_{ij} = B_{ij}c_{ii} - B_{ij}c_{ij} - G_{ij}s_{ij} \qquad \forall (i,j)\in\mathcal{L} \tag{4c}$$
$$\sum_{g\in\mathcal{G}_i} p_g - p_i^d = (G_{ii} + \sum_{j\in\delta_i} G_{ij})c_{ii} + \sum_{j\in\delta_i} p_{ij} \quad \forall i\in\mathcal{N} \tag{4d}$$
$$\sum_{g\in\mathcal{G}_i} q_g - q_i^d = -(B_{ii} + \sum_{j\in\delta_i} B_{ij})c_{ii} + \sum_{j\in\delta_i} q_{ij} \;\forall i\in\mathcal{N} \tag{4e}$$
$$(V_i^{min})^2 \le c_{ii} \le (V_i^{max})^2 \qquad \forall i\in\mathcal{N} \tag{4f}$$
$$c_{ij} = c_{ji}\ ,\ s_{ij} = -s_{ji} \qquad \forall (i,j)\in\mathcal{L} \tag{4g}$$
$$\left\| \begin{matrix} 2c_{ij} \\ 2s_{ij} \\ c_{ii} - c_{jj} \end{matrix} \right\| \le c_{ii} + c_{jj} \qquad \forall (i,j)\in\mathcal{L} \tag{4h}$$
$$(1g), (1h), (1i)$$

The presented SOCP relaxation formulation in (4) is exact for radial networks, so the procured solution to the relaxed problem is the same as the one procured by the original non-convex problem and the voltage angles can be recovered with any choice of a reference bus. However, this relaxation is not exact for a general mesh network with multiple cycles. The main issue with the relaxation presented in (4) is the absence of constraints enforcing the voltage angles across the network. In other words, recovering the voltage angles from the presented relaxation is not straightforward. Unique angle differences cannot be procured unless it is enforced in the SOCP relaxation formulation. Therefore, the cycle constraint presented in (5a) should be added to the SOCP problem formulation to guarantee that the voltage angle difference of buses in a cycle sums to zero. Thus, voltage angles may be recovered by enforcing the non-convex constraint presented in (5a), where the lifting terms c_{ij} and s_{ij} are utilized to recover the difference in voltage angles of a pair of buses. Adding the presented constraint in (5) will make the convex relaxation problem presented in (4) non-convex. Thus, in the next subsection, a set of valid constraints is presented to preserve the relationship enforced in (5) and avoid a non-convex problem formulation.

$$\theta_{ij} = \theta_i - \theta_j = atan2(s_{ij}, c_{ij}) \qquad (i,j)\in\mathcal{L} \tag{5a}$$
$$atan2(s_{ij}, c_{ij}) = \begin{cases} arctan(\frac{s_{ij}}{c_{ij}}) & ; c_{ij} > 0 \\ arctan(\frac{s_{ij}}{c_{ij}}) + \pi & ; s_{ij} \ge 0, c_{ij} < 0 \\ arctan(\frac{s_{ij}}{c_{ij}}) - \pi & ; s_{ij} < 0, c_{ij} < 0 \\ +\frac{\pi}{2} & ; s_{ij} > 0, c_{ij} = 0 \\ -\frac{\pi}{2} & ; s_{ij} < 0, c_{ij} = 0 \\ undefined & ; s_{ij} = 0, c_{ij} = 0 \end{cases} \tag{5b}$$

C. Non-Convex Cycle Constraints

This subsection aims to present a set of valid constraints to be utilized in place of the non-convex angle constraint given in (5). To this end, the three buses of an arbitrary cycle shown in Fig. 1 are referred to as bus i, j, and k. The summation of the voltage angle difference of the pair of buses within a cycle is zero as shown in (6a). Applying the cos operator to both

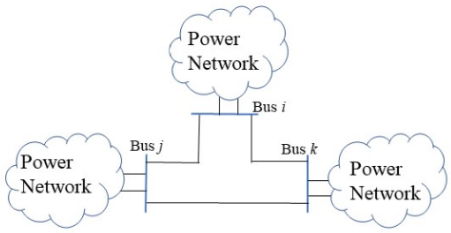

Fig. 1. An arbitrary cycle with three buses in a mesh network

sides of the equation presented in (6a) results in the equation presented in (6b). The expanded form of the argument of the cos function in (6b) is given in (6c), where the right-hand side is 1 and the left-hand side is composed of four terms of trigonometric multiplications which are non-convex.

$$\theta_{ij} + \theta_{jk} + \theta_{ki} = 0 \tag{6a}$$

$$\cos\left(\theta_{ij} + \theta_{jk} + \theta_{ki}\right) = \cos\left(0\right) \tag{6b}$$

$$\begin{pmatrix} \cos\theta_{ij}\cos\theta_{jk}\cos\theta_{ki} - \sin\theta_{ij}\sin\theta_{jk}\cos\theta_{ki} \\ -\sin\theta_{ij}\cos\theta_{jk}\sin\theta_{ki} - \cos\theta_{ij}\sin\theta_{jk}\sin\theta_{ki} \end{pmatrix} = 1 \tag{6c}$$

The non-convex terms in the left-hand side of the (6c) are undesirable. In (7), both side of the equation presented in (6c) are multiplied by $(|V_i|\,|V_j|\,|V_k|)^2$.

$$\begin{pmatrix} (|V_i|\,|V_j|\cos\theta_{ij})(|V_j|\,|V_k|\cos\theta_{jk})(|V_k|\,|V_i|\cos\theta_{ki}) \\ -(|V_i|\,|V_j|\sin\theta_{ij})(|V_j|\,|V_k|\sin\theta_{jk})(|V_k|\,|V_i|\cos\theta_{ki}) \\ -(|V_i|\,|V_j|\sin\theta_{ij})(|V_j|\,|V_k|\cos\theta_{jk})(|V_k|\,|V_i|\sin\theta_{ki}) \\ -(|V_i|\,|V_j|\cos\theta_{ij})(|V_j|\,|V_k|\sin\theta_{jk})(|V_k|\,|V_i|\sin\theta_{ki}) \end{pmatrix} = (|V_i|\,|V_i|)(|V_j|\,|V_j|)(|V_k|\,|V_k|) \tag{7}$$

As the non-linear and non-convex terms presented in (7) are not desirable, they can be represented in the form presented in (8).

$$\begin{pmatrix} \mathbf{Re}\{V_i^*V_j\}\mathbf{Re}\{V_j^*V_k\}\mathbf{Re}\{V_k^*V_i\}) \\ -\mathbf{Im}\{V_i^*V_j\}\mathbf{Im}\{V_j^*V_k\}\mathbf{Re}\{V_k^*V_i\} \\ -\mathbf{Im}\{V_i^*V_j\}\mathbf{Re}\{V_j^*V_k\}\mathbf{Im}\{V_k^*V_i\} \\ -\mathbf{Re}\{V_i^*V_j\}\mathbf{Im}\{V_j^*V_k\}\mathbf{Im}\{V_k^*V_i\} \end{pmatrix} = V_i^*V_iV_j^*V_jV_k^*V_k \tag{8}$$

Applying the lifting terms, c_{ii}, c_{ij}, and s_{ij} introduced in (2), equality given in (8) is represented as given in (9a). The constraint presented in (9a) is further represented in a compact form as given in (9b). Enforcing constraint given in (9b) will ensure that the summation of angle differences of pair of buses within a cycle is zero. However, this equation renders tri-linear terms which are also non-convex and still undesirable.

$$\begin{pmatrix} c_{ij}c_{jk}c_{ki} - s_{ij}s_{jk}c_{ki} - \\ s_{ij}c_{jk}s_{ki} - c_{ij}s_{jk}s_{ki} \end{pmatrix} = c_{ii}c_{jj}c_{kk} \tag{9a}$$

$$\begin{pmatrix} c_{ij}(c_{jk}c_{ki} - s_{jk}s_{ki}) - \\ s_{ij}(s_{jk}c_{ki} + c_{jk}s_{ki}) \end{pmatrix} = c_{ii}c_{jj}c_{kk} \tag{9b}$$

The constraints procured in (9) are not desirable and are not utilized in this work. A different take on the equation presented in (6a) will pave the way to come up with some desirable terms. In a cycle similar to the one in Fig.1 with three buses, the voltage angle difference of a pair of buses within a cycle is equal to the negative sum of the other two pairs of buses: $\theta_{ij} = -(\theta_{jk} + \theta_{ki})$. Applying the sin and cos operator will lead to: $sin\ \theta_{ij} = sin(-(\theta_{jk} + \theta_{ki}))$ and $cos\ \theta_{ij} = cos(-(\theta_{jk} + \theta_{ki}))$. Expanding the argument of the trigonometric terms will result in the form presented in (10). Similar to equations (7)-(8), multiplying the two trigonometric equations by $|V_i|\,|V_j|\,|V_k|^2$ will lead to the form presented in (11). Then, leveraging the lifting terms introduced in (2), the phasor form presented in (11) is reformulated into the form presented in (12). Here, the equations procured in (12) are the equivalent of the one presented in (9). Although the terms procured in (12) are bilinear, their level of non-convexity is less complicated than the tri-linear terms presented in (9).

$$\begin{cases} \sin\theta_{ij} = -\sin\theta_{jk}\cos\theta_{ki} - \cos\theta_{jk}\sin\theta_{ki} \\ \cos\theta_{ij} = \cos\theta_{jk}\cos\theta_{ki} - \sin\theta_{jk}\sin\theta_{ki} \end{cases} \tag{10}$$

$$\begin{cases} \mathbf{Im}\{(V_i^*V_j)(V_k^*V_k)\} = -\mathbf{Im}\{(V_j^*V_k)(V_k^*V_i)\} \\ \mathbf{Re}\{(V_i^*V_j)(V_k^*V_k)\} = \mathbf{Re}\{(V_j^*V_k)(V_k^*V_i)\} \end{cases} \tag{11}$$

$$\begin{cases} s_{ij}c_{kk} = -c_{jk}s_{ki} - s_{jk}c_{ki} \\ c_{ij}c_{kk} = c_{jk}c_{ki} - s_{jk}s_{ki} \end{cases} \tag{12}$$

A unique solution can be procured using (5a) if summations of voltage angle differences over cycles are zero and (12) is enforcing this condition. Thus, satisfying the constraints presented in (12) is equivalent to satisfying the non-convex constraint presented in (5a). However, the procured constraints are still non-convex. While McCormick-based LP Relaxation and arctangent envelopes are employed in [23], in the next subsection, a convex relaxation approach based on a higher-order SOCP relaxation of the bi-linear terms of (12) is presented.

D. Cycle Constraint Convex Relaxation

To present the non-convex constraints given in (12) in a convex form, its phasor form presented in (11) is taken into account. A new set of lifting terms should be introduced to remedy the non-convexity of the bi-linear terms in (12). The new set of lifting terms should be defined over the multiplication of voltage phasors within a cycle. To this end, the *sparse second-order moment relaxation matrix associated with each maximal clique of the chordal extended graph of the network* is introduced. Reviewing several graph theoretic definitions is necessary to proceed with the discussion. A clique is a subset of the graph vertices for which each vertex in the clique is connected to all other vertices in the clique. A maximal clique is a clique that is not a proper subset of another clique. A graph is chordal if each cycle of length four or more vertices has a chord, which is an edge connecting two vertices that are not adjacent in the cycle.

The chordal extension of the graph associated with the 5-bus network is presented in Fig. 2 to enable the formation of the second-order moment relaxation matrix of the terms employed in the SOCP relaxation method. In Fig. 2, the chord 2-4 is added to the graph of the 5-bus network to obtain the chordal extended graph of the 5-bus network. This will also make the size of all cycles equal to 3, which is suitable for the convex relaxation of the cycle constraints. Once the chordal extension is applied, the maximal cliques of this network are (1,5,4), (1,2,4), and (2,3,4). Here, the size of a cycle and clique

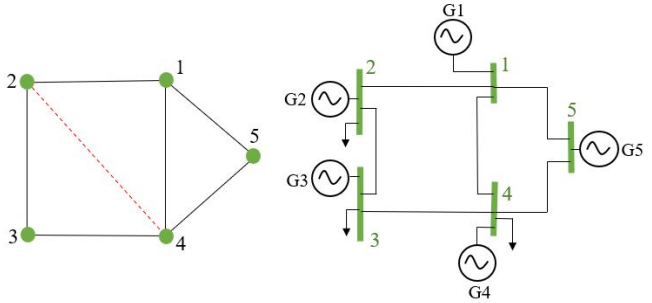

Fig. 2. Chordal extended graph of a 5-bus network

is referred to the total number of its vertices. Therefore, the extended graph of power network contains cycles with three buses as given in Fig. 1.

1) First-Order Moment Formulation: To enable the definition of the moment matrix in its sparse form, the graph of the network should be chordal [17]. The chordal extension will add a chord to any cycle of length more than 3, so the chordal extended graph will only have cycles with three buses as assumed in the previous subsection. However, these cycles with 3 pairs of buses may include those virtually added chords. Once the chordal extension is done, the maximal cliques of the graph associated with the chordal extended network are procured.

Once the maximal cliques of the chordal extended graph of the network are established, the first-order moment relaxation matrix associated with each maximal clique can be formulated using the basis given in (13) and its conjugate.

$$v_c = \begin{bmatrix} V_i & V_j & \dots & V_{|c|} \end{bmatrix} \tag{13}$$

$$W_c^{\alpha} = v_c^* v_c = \begin{bmatrix} V_i^*V_i & V_i^*V_j & \dots & V_i^*V_{|c|} \\ V_j^*V_i & V_j^*V_j & \dots & V_j^*V_{|c|} \\ . & . & & . \\ . & . & & . \\ . & . & & . \\ V_{|c|}^*V_i & V_{|c|}^*V_j & \dots & V_{|c|}^*V_{|c|} \end{bmatrix} \tag{14a}$$

$$V_i^*V_j \xrightarrow{lifting} \gamma(V_i^*V_j) \equiv \gamma_{V_i^*V_j} \tag{14b}$$

The relationship between the moment relaxation matrix and its basis is presented in (14a), using the basis presented in (13) and its conjugate. The lifting operator is illustrated in (14b) to relax the bilinear elements of the matrix presented in (14a). Note that for convenience, the lifting operator is rewritten as lifting variable γ with the associated lifted bilinear term as its subscript. Therefore, by replacing the bilinear elements of the matrix given in (14a) with their related lifting variables, the first-order moment relaxation matrix given in (15) is obtained. However, the rank-1 constraint given in (14a) is non-convex. Furthermore, the quadrilateral terms in (11) are not presented in the first-order moment relaxation given in (15). Thus, the second-order moment relaxation matrix is formed in the next part to procure those terms.

$$W_c = \begin{bmatrix} \gamma_{V_i^*V_i} & \gamma_{V_i^*V_j} & \dots & \gamma_{V_i^*V_{|c|}} \\ \gamma_{V_j^*V_i} & \gamma_{V_j^*V_j} & \dots & \gamma_{V_j^*V_{|c|}} \\ . & . & & . \\ . & . & & . \\ . & . & & . \\ \gamma_{V_{|c|}^*V_i} & \gamma_{V_{|c|}^*V_j} & \dots & \gamma_{V_{|c|}^*V_{|c|}} \end{bmatrix} \tag{15}$$

The relationship between the lifting terms introduced for the SOCP relaxation problem formulation in (2) and the lifting variables given in (14b) is presented in (16).

$$c_{ii} = \gamma_{V_i^*V_i} \tag{16a}$$

$$c_{ij} = \mathbf{Re}\{\gamma_{V_i^*V_j}\} \tag{16b}$$

$$s_{ij} = \mathbf{Im}\{\gamma_{V_i^*V_j}\} \tag{16c}$$

2) Second-Order Moment Relaxation Formulation: The equivalent cycle constraints presented in (11) contain quadrilateral voltage phasor terms. To obtain the relaxed form of these terms, the second-order moment relaxation matrix definition is employed. The basis of the second-order moment relaxation matrix is given in (17) which includes the elements of the first-order moment relaxation matrix given in (15).

$$v_c' = \begin{bmatrix} v_c & \gamma_{V_i^*V_i} & \gamma_{V_i^*V_j} & \dots & \gamma_{V_{|c|}^*V_{|c-1|}} & \gamma_{V_{|c|}^*V_{|c|}} \end{bmatrix} \tag{17}$$

The non-convex rank-1 constraint of the second-order moment relaxation matrix of each maximal clique is given in (18a).

$$W^{\alpha'}{}_c = v_c'^* v_c' \tag{18a}$$

$$V_i^*V_kV_k^*V_j \xrightarrow{lifting} \gamma(V_i^*V_kV_k^*V_j) \equiv \gamma_{V_i^*V_kV_k^*V_j} \tag{18b}$$

Similar to the first order moment relaxation matrix presented in (15), the second-order moment relaxation is presented using the lifting terms. A set of lifting variables is introduced in (18b) to relax the bilinear elements of the matrix $W^{\alpha'}{}_c$ presented in (18a). By relaxing the elements of the matrix $W^{\alpha'}{}_c$ presented in (18a) with the set of lifting variables introduced in (18b) the second-order moment relaxation matrix W_c' is rendered as shown in (19).

$$W_c' = \begin{bmatrix} \gamma_{|V_i|^2} & \dots & \gamma_{V_i^*V_{|c|}} & \gamma_{V_i^*|V_i|^2} & \dots & \gamma_{V_i^*|V_{|c|}|^2} \\ . & & . & . & & . \\ . & & . & . & & . \\ . & & . & . & & . \\ \gamma_{V_{|c|}^*V_i} & \dots & \gamma_{|V_{|c|}|^2} & \gamma_{V_{|c|}^*|V_i|^2} & \dots & \gamma_{V_{|c|}^*|V_{|c|}|^2} \\ \gamma_{|V_i|^2V_i} & \dots & \gamma_{|V_i|^2V_{|c|}} & \gamma_{|V_i|^4} & \dots & \gamma_{|V_i|^2|V_{|c|}|^2} \\ . & & . & . & & . \\ . & & . & . & & . \\ . & & . & . & & . \\ \gamma_{|V_{|c|}|^2V_i} & \dots & \gamma_{|V_{|c|}|^2V_{|c|}} & \gamma_{|V_{|c|}|^2|V_i|^2} & \dots & \gamma_{|V_{|c|}|^4} \end{bmatrix} \tag{19}$$

The second-order elements of the second-order moment relaxation matrix W_c' are the relaxed form of the quadrilateral terms, so the conic constraint (3d) and the cycle constraint (11) can be represented in form given in (20). Here, the equation (20a) holds for each pair of buses in the chordal

extended network. The relaxed form of the cycle constraint presented in (20b) holds for each cycle of three buses within the chordal extended network. The two sides of the relaxed cycle constraint presented in (20b) are explicitly related by enforcing this constraint. However, as the rank-1 constraint presented in (18a) is non-convex, the lifting terms inside the moment relaxation matrix W_c' should be presented in a conic relaxation form. A computationally efficient conic relaxation is presented in the next subsection.

$$\mathbf{Re}\{\gamma_{(V_i^*V_j)^2}\} + \mathbf{Im}\{\gamma_{(V_i^*V_j)^2}\} = \gamma_{(V_i^*V_i)(V_j^*V_j)} \tag{20a}$$

$$\begin{cases} \mathbf{Re}\{\gamma_{(V_i^*V_j)(V_k^*V_k)}\} = \mathbf{Re}\{\gamma_{(V_j^*V_k)(V_k^*V_i)}\} \\ \mathbf{Im}\{\gamma_{(V_i^*V_j)(V_k^*V_k)}\} = -\mathbf{Im}\{\gamma_{(V_j^*V_k)(V_k^*V_i)}\} \end{cases} \tag{20b}$$

E. The Proposed Conic Relaxation

The moment relaxation matrix W_c' is associated with each maximal clique of the network. Enforcing the elements of the second-order moment relaxation matrix in a semi-definite cone has computation complexity of $\mathcal{O}(2(|c|(1+|c|/2))^3)$ which is proportional to the largest clique within the network. Thus, a computationally less demanding second-order cone is utilized here with the computational complexity of $\mathcal{O}(2)^3$. The second-order cone constraints are presented for each 2×2 principal minors of the second-order moment relaxation matrix as given in (21), where $W_c'(i,j)$ is the element ith row and jth column of the second-order moment relaxation matrix. Knowing the relationship between SOCP relaxation lifting variables and first-order moment relaxation lifting variables in (16), one can rewrite the SOC constraint given in (4f) in the form presented in (21a). The relationship between lifting terms presented in (4g) is also reformulated as (21b) and (21c).

$$\left\| \begin{matrix} 2\mathbf{Re}\{W_c'(i,j)\} \\ 2\mathbf{Im}\{W_c'(i,j)\} \\ W_c'(i,i) - W_c'(j,j) \end{matrix} \right\| \leq W_c'(i,i) + W_c'(j,j) \tag{21a}$$

$$\mathbf{Re}\{W_c'(i,j)\} = \mathbf{Re}\{W_c'(j,i)\} \tag{21b}$$

$$\mathbf{Im}\{W_c'(i,j)\} = -\mathbf{Im}\{W_c'(j,i)\} \tag{21c}$$

Similarly, constraints (4b) - (4f) are represented in the form given in (22).

$$\begin{cases} p_{ij} = -G_{ij}\mathbf{Re}\{\gamma_{V_i^*V_i}\} \\ +G_{ij}\mathbf{Re}\{\gamma_{V_i^*V_j}\} - B_{ij}\mathbf{Im}\{\gamma_{V_i^*V_j}\} \end{cases} \quad \forall (i,j) \in \mathcal{L} \tag{22a}$$

$$\begin{cases} q_{ij} = B_{ij}\mathbf{Re}\{\gamma_{V_i^*V_i}\} \\ -B_{ij}\mathbf{Re}\{\gamma_{V_i^*V_j}\} - G_{ij}\mathbf{Im}\{\gamma_{V_i^*V_j}\} \end{cases} \quad \forall (i,j) \in \mathcal{L} \tag{22b}$$

$$\begin{cases} \sum_{g\in\mathcal{G}_i} p_g - p_i^d = \sum_{j\in\delta_i} p_{ij} \\ +(G_{ii} + \sum_{j\in\delta_i} G_{ij})\mathbf{Re}\{\gamma_{V_i^*V_i}\} \end{cases} \quad \forall i \in \mathcal{N} \tag{22c}$$

$$\begin{cases} \sum_{g\in\mathcal{G}_i} q_g - q_i^d = \sum_{j\in\delta_i} q_{ij} \\ -(B_{ii} + \sum_{j\in\delta_i} B_{ij})\mathbf{Re}\{\gamma_{V_i^*V_i}\} \end{cases} \quad \forall i \in \mathcal{N} \tag{22d}$$

$$(V_i^{min})^2 \leq \gamma_{V_i^*V_i} \leq (V_i^{max})^2 \quad \forall i \in \mathcal{N} \tag{22e}$$

Once all the SOCP relaxation lifting variables given in (2) replaced by the lifting variables introduced in (14b), the cycle constraint relaxation (CCR) of the AC-OPF problem given in (1) is presented in (23).

$$\begin{aligned} &\min \sum_{g\in\mathcal{G}} C_g(P_g) \\ &\text{s.t.} \qquad (1g) - (1i), (20), (21), (22) \end{aligned} \tag{23}$$

Note that the optimization variables of the CCR relaxation problem presented in (23) are the elements of the W_c' matrix introduced in (19). The elements of sparse second-order moment relaxation matrix are employed to enforce cycle constraints. This adds a set of valid constraints *representing the cycle constraints* which will present additional cuts to the feasible region of the relaxation problem to achieve an optimal solution that is tighter than the one procured by the SOCP relaxation problem. However, the procured solution by the CCR problem formulation is not as tight as utilizing the semi-definite relaxation of the second-order moment relaxation matrix.

F. Checking The Relaxation Tightness

One measure to check the gap between the proposed method and the original problem is the difference of objective values divided by the objective value of the original problem. In [30], the difference between the objective values of each method and the original problem divided by the objective value of the original problem is considered a gap of the proposed method. Another approach leverages the ratio of the largest and the second largest eigenvalue of the moment relaxation matrices associated with each maximal clique as suggested in [31], [32]. In the SOCP relaxation formulation, the constraint presented in (3d) replaced by its conic relaxation form given in (4h). Therefore an alternative approach to check the tightness of the procured relaxation scheme is the difference between $c_{ij}^2 + s_{ij}^2$ and $c_{ii}c_{jj}$. The presented relaxation tightness measure employed here is based on the relaxed terms in the SOCP relaxation in which $c_{ij}^2 + s_{ij}^2 = c_{ii}c_{jj}$ is replaced by its conic relaxation form. In a radial network, the relaxation is exact because the angles can be uniquely identified by an arbitrary reference voltage. If the summation of angle differences of bus-pairs over a cycle is zero, such a unique relationship can be procured. Here, the term utilized in (24) indicates the gap in the relaxation of the equation in (3d) to the SOCP form given in (4h). If the difference is zero, it means that the relaxation is exact. However, in practice, due to numerical precious issues, the gap might not be exactly zero, but it can be close enough to render a good quality solution. Therefore, this gap indicator is employed in the algorithm as a measure of exactness for the procured solution from the convex relaxation problem. Since this differential value is small and near to zero so the relaxation tightness is the minus of logarithmic value. The measure for the tightness of the solution procured from is the minus of logarithmic value of the difference between $c_{ij}^2 + s_{ij}^2$ and $c_{ii}c_{jj}$, where $\mathcal{RT}$ is the tightness measure for each pair i, j and $c_{ii}, c_{jj}, c_{ij}, s_{ij}$ associated with pair i, j.

$$\mathcal{RT}_{ij} = -\log\left|c_{ij}^2 + s_{ij}^2 - c_{ii}c_{jj}\right| \tag{24}$$

G. Angle Recovery

As the relaxation gap may lead to an inexact solution, calculating unique voltage angles by plugging the procured solution of (23) into (5) is challenging. The procured voltage magnitudes as well as *inaccurate* voltage angle differences from CCR solution can be used as a warm start point for a non-linear optimization problem solved by interior-point solvers, so a feasible solution can be procured. As the relaxation gap is small, the first-order Taylor approximation is utilized in this

Section. If the voltage angle is approximated and all other constraints of SOCP relaxation presented in (4) are satisfied, a solution can be recovered. Therefore, the first-order Taylor approximation is employed to approximate c_{ij}, s_{ij}.

$$c_{ij} \simeq \widehat{c}_{ij} + \frac{\partial c_{ij}}{\partial v_i}(v_i - \widehat{v}_i) + \frac{\partial c_{ij}}{\partial v_j}(v_j - \widehat{v}_j) + \frac{\partial c_{ij}}{\partial \theta_{ij}}(\theta_{ij} - \widehat{\theta}_{ij}) \tag{25a}$$

$$s_{ij} \simeq \widehat{s}_{ij} + \frac{\partial s_{ij}}{\partial v_i}(v_i - \widehat{v}_i) + \frac{\partial s_{ij}}{\partial v_j}(v_j - \widehat{v}_j) + \frac{\partial s_{ij}}{\partial \theta_{ij}}(\theta_{ij} - \widehat{\theta}_{ij}) \tag{25b}$$

Using c_{ij}, s_{ij} definition presented in (2) and Taylor approximation (25) leads to a new set of c_{ij}, s_{ij}. Running a post AC power flow with the constraints of CCR formulation excluding (21) and the two constraints obtained from the first-order Taylor approximation gives new voltage angles. Note that the decision variables in the angle recovery post optimization problem are $p_{ij}, q_{ij}, p_g, q_g, \theta_{ij}, v_i$.

$$\min \sum_{g\in\mathcal{G}} C_g(p_g) \tag{26a}$$

$$\text{s.t.} \quad c_{ij} = \widehat{v}_j cos\widehat{\theta}_{ij}(v_i - \widehat{v}_i) + \widehat{v}_i cos\widehat{\theta}_{ij}(v_j - \widehat{v}_j) - \widehat{v}_i\widehat{v}_j sin\widehat{\theta}_{ij}(\theta_{ij} - \widehat{\theta}_{ij}) + \widehat{c}_{ij} \tag{26b}$$

$$s_{ij} = \widehat{v}_j sin\widehat{\theta}_{ij}(v_i - \widehat{v}_i) + \widehat{v}_i sin\widehat{\theta}_{ij}(v_j - \widehat{v}_j) + \widehat{v}_i\widehat{v}_j cos\widehat{\theta}_{ij}(\theta_{ij} - \widehat{\theta}_{ij}) + \widehat{s}_{ij} \tag{26c}$$

$$(1g), (1h), (1i), (4b), (4c), (4d), (4e), (4f), (4g) \tag{26d}$$

IV. Case Study

To show the merit of the proposed cycle constraint relaxation on the optimal power flow problem, several case studies are presented. Also, the tightness of the procured solution is compared with the one procured by the second-order cone and sparse second-order semi-definite relaxation methods. Here, Mosek [33] is employed as the off-the-shelf solver to solve conic programming problem formulations. The results presented here are performed on a PC with Core i7 CPU 4.70GHz processor and 48 GB memory. Comparing the optimality gap of utilizing various algorithms reveals that the solution procured by the SOCP relaxation is not always feasible with a zero optimality gap. Furthermore, it is shown that the gap presented by the CCR method is diminished compared to the optimality gap of the solution procured by the SOCP relaxation method. In each case, it is shown that the presented CCR-OPF approach can render a solution with an enhanced tightness compared to the SOCP relaxation with a computation burden much less than the SDP relaxation method. Another measure to evaluate the exactness of a convex optimization method is comparing their optimality gap. The optimality gap introduced as the difference between the objective value obtained from solving the nonlinear original OPF problem with IPOPT [34] as the best known feasible point for the non-convex AC-OPF problem and the objective value obtained from solving the relaxed form of OPF problem with Mosek [33] as a conic solver [8].

$$Gap\% = \frac{Obj_{nonlinear} - Obj_{relaxation}}{Obj_{nonlinear}} \times 100 \tag{27}$$

The optimality gap measure presented in (27) shows the difference between the objective value of the solution procured by the convex relaxation method as the lower bound and the upper bound solution procured by solving the non-convex original OPF problem. It should be noted that comparing the optimality gap calculated for each relaxation approach is not an indicator to determine if the solution that procured by each method is feasible for the original non-convex problem. However, along with the tightness measures introduced in subsection III-F it can render a comparison of the relaxation schemes.

A. IEEE 14-Bus System

In this subsection, the IEEE 14-bus system is considered as a test case. IEEE 14-bus system consists of 20 lines, 5 generators, 3 transformers, and 11 loads as shown in Fig. 3.

A comparison of mean, maximum, standard deviation, median, and minimum values of tightness are presented in Table I given the tightness values of all bus-pairs with a finite tightness. Comparing the mean and median values of the tightness measures in Table I obtained from each method shows that the tightness measure of the CCR method is slightly improved compared to that of SOCP relaxation method. However, these comparisons reveal limited information on the merit of the proposed relaxation scheme in this paper to enforce the cycle constraints within the network. Therefore, the recovered voltage angles difference for each bus-pair of the network using CCR and SOCP relaxation methods are employed to calculate the summation of angle differences within each cycle of the network as shown in Table II. The network has 7 cycles

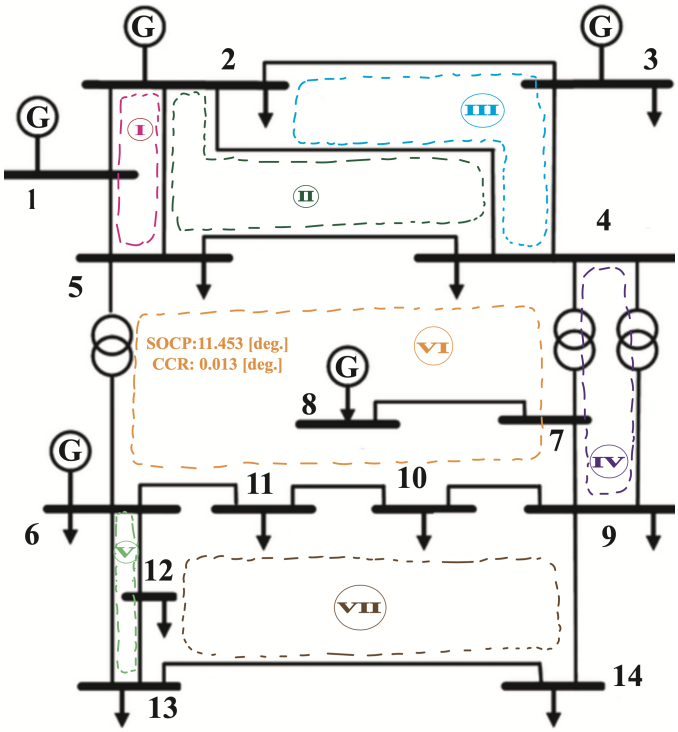

Fig. 3. The one-line diagram of IEEE-14 bus system with seven marked cycles within the network

as listed in Table II and noted in Fig. 3. It is interesting to observe that the summation of angle difference each cycle utilizing the CCR method is is smaller than that of employing the SOCP relaxation. This is particularly notable in cycle IV, where the mismatch in angles within the cycle is 11.453° using the SOCP relaxation method while that is 0.013° when the CCR method is employed. Thus, by employing the CCR method, the mismatch of the voltage angle constraint presented in (6b) is smaller than the one procured by employing the SOCP relaxation method.

Comparing the objective value, the solution time, and the optimality gap of each method is another way to compare the performance of various solution methods. In Table III, the objective values, the solution time, and the optimality gap of each relaxation method are presented. The solution time of the CCR method is less than that for the sparse SDP method, which means that the computational burden of the CCR method is less than that of the SDP relaxation method. The objective value of the CCR relaxation problem is less than that obtained from the sparse SDP relaxation method and more than the objective value procured by the SOCP relaxation method. The optimality gap of the presented CCR method is slightly larger than that of the solution procured by the SDP relaxation method and smaller than that of the one procured by the SOCP relaxation method.

B. 500-Bus System

In this section, a modified 500-bus system presented in [35] is considered as a test case. The 500-bus system consists of 599 lines, 90 generators, 131 transformers, and 200 loads.

1) Base Case: In this setup, similar to the IEEE 14-bus system test case, the tightness and performance of the CCR method are compared with the SOCP and the SDP relaxation methods.The tightness of the solutions procured by each method is compared in Table IV. Comparing the number of pairs with zero gap in Table IV illustrates that 8 bus-pairs have zero gaps when the CCR method is employed, but this number is 3 and 6 when the SOCP and SDP relaxation methods are employed, respectively. The number of zero-gap pairs gives the number of bus-pairs in which the equality constraint (3d) holds while only enforcing the conic constraints (4h) or (21a), i.e. the relaxation is exact for the bus-pair. The mean, maximum, standard deviation, median, and minimum values of the tightness measure presented in Table IV are obtained from the tightness values of all bus-pairs with a finite tightness measure. An interesting observation is a higher mean and median value of finite tightness measures for the CCR method compared to SOCP and SDP relaxation methods.

TABLE I
THE COMPARISON OF THE TIGHTNESS MEASURES' STATISTICS WITH VARIOUS RELAXATION METHODS FOR IEEE 14-BUS SYSTEM

Tightness Measure	**SOCP**	**SDP**	**CCR**
Mean	15.7	15.87	15.84
Maximum	16.91	17.158	16.68
Standard Deviation	0.413	0.526	0.498
Median	15.59	15.76	15.73
Minimum	15.23	15.256	15.13
Number of Zero Gap Pairs	0	0	0

TABLE II
THE COMPARISON OF ANGLE DIFFERENCE SUMMATION OVER CYCLES OF IEEE 14-BUS SYSTEM EMPLYING SOCP AND CCR METHODS

Cycle ID	**Cycle's Bus Sequence**	**SOCP**	**CCR**
I	1-2-5	0.389°	$7\times10^{-6\circ}$
II	2-5-4	0.046°	$4.8\times10^{-6\circ}$
III	2-4-3	1.886°	$3\times10^{-6\circ}$
IV	7-4-9	0.441°	0.261°
V	6-12-13	0.086°	$3.6\times10^{-6\circ}$
VI	**5-6-11-10-9-4**	$\mathbf{11.453^\circ}$	$\mathbf{0.013^\circ}$
VII	6-13-14-9-10-11	0.142°	$1.8\times10^{-6\circ}$

TABLE III
THE COMPARISON OF OBJECTIVE VALUES AND SOLUTION TIMES OF USING VARIOUS RELAXATION METHODS FOR IEEE 14-BUS SYSTEM

	SOCP	**SDP**	**CCR**
Objective Value [$]	14,666.9	14,676.9	14,676.1
Solution Time [Sec.]	0.021	0.172	0.046
Optimality Gap [%]	0.07004	0.00191	0.00735

TABLE IV
THE COMPARISON OF THE TIGHTNESS MEASURES' STATISTICS WHEN USING VARIOUS RELAXATION METHODS FOR 500-BUS SYSTEM

Tightness Measure	**SOCP**	**SDP**	**CCR**
Mean	15.82	15.77	15.90
Maximum	17.88	18.13	17.88
Standard Deviation	0.46	0.42	0.43
Median	15.71	15.69	15.75
Minimum	15.13	15.1	15.07
Number of Zero Gap Pairs	3	6	8

In Table V, the objective values, the solution time, and the optimality gap of each method are presented. The objective value procured by the CCR method is more than that obtained from the SOCP relaxation method. The optimality gap of the solution procured by the CCR relaxation method is less than that obtained from the SOCP method while the solution time of the CCR relaxation method is less than that of the SDP relaxation method. Given the results of tightness from Table IV and the performance of each method obtained from Table V, one can conclude that the CCR method has a solution time, less than SDP relaxation method and a solution with an enhanced tightness compared to the SOCP relaxation method. In this case, the average of summation of angle differences of buses over cycles procured by the SOCP relaxation method is 0.66° and it is 27.3% reduced to 0.48° when the CCR relaxation method is employed.

TABLE V
THE COMPARISON OF OBJECTIVE VALUES AND SOLUTION TIMES OF USING VARIOUS RELAXATION METHODS FOR 500-BUS SYSTEM

	SOCP	**SDP**	**CCR**
Objective Value [$]	31,886	32,137	31,913
Solution Time [Sec.]	0.625	33.37	2.64
Optimality Gap [%]	2.0	1.2	1.9

2) Day-Ahead Case: Here, the day-ahead performance and effectiveness of the proposed CCR method are compared with the SOCP relaxation method. The results are shown in Figs. 4, 5, and 6. The base demand is set according to the normalized hourly load of California ISO on March 10, 2020. An interesting observation is that for the same system, changes in the demand throughout a day exhibit various tightness and performance measures for various algorithms. However, the

improvements in employing the CCR method compared to the SOCP relaxation is consistent with those variations.

It is shown in Fig. 4 that optimality gap is improved while employing the CCR method compared to employing the SOCP relaxation method, i.e. the optimality gap of the CCR method is at worst the same as the one for SOCP relaxation method e.g. hours 4-18. However, there are hours in which the optimality gap is notably reduced by employing the CCR method e.g. hours 19 and 20. Enforcing the cycle constraints in the CCR relaxation method leads to a smaller optimality gap and a better quality solution in the day-ahead case. Note that the optimality gap improvement is the subtraction of the optimality gap of the solution procured by the CCR method from the one procured by the SOCP relaxation method, divided by the optimality gap of the solution procured by the SOCP relaxation method. The comparison of the solution time for various methods in Fig. 5 reveals that although the solution time of the CCR method is greater than that of the SOCP relaxation method, it is still much smaller than that in the sparse SDP relaxation method. The number of exact bus-pairs, as well as the mean of tightness measures of bus-pairs for the SOCP and CCR relaxation methods, are compared in Fig. 6. It should be noted that a combination of these two values should be taken into account while comparing the tightness of employing the two methods. If a larger number of bus-pairs are exact for the CCR method, the median of the remaining inexact bus-pairs could be smaller than that of the SOCP relaxation method. This is because the exact bus-pairs of the CCR method could already have large tightness measure values employing the SOCP relaxation method. For example, at hour 1, when the CCR method is employed, there are three more bus-pairs with zero gap compared to the SOCP relaxation method while the median of relaxation tightness measure is slightly smaller using the CCR method. The optimality gap of the solution of a relaxation method shows the tightness of the objective value of the solution, while the RT measure shows the quality of the solution procured by the relaxation method i.e. the possibility of recovering a feasible solution from the relaxed solution. Fig. 6 and 4 illustrate that when the solution procured by the CCR method has comparable optimality gap as the one procured by the SOCP method, the quality of the solution procured by the CCR method is mostly better than the one procured by the SOCP method as shown in hours 12 and 13. Moreover, when the optimality gap of the solution procured by the CCR method is less than that procured by the SOCP method, the solutions procured by both methods have a comparable quality as shown in hours 19 and 20.

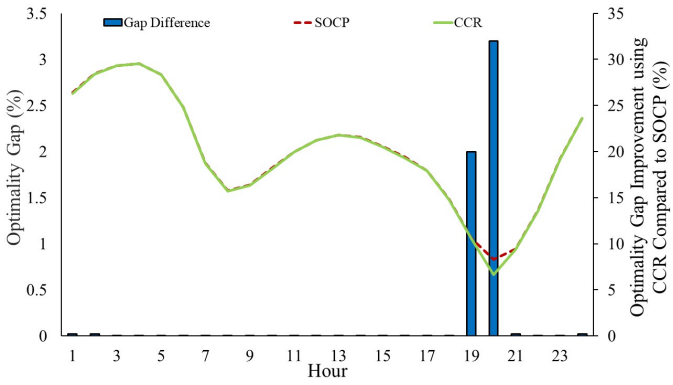

Fig. 4. The reduction in optimality gap of SOCP relaxation method by implementing CCR relaxation method for 500-bus system

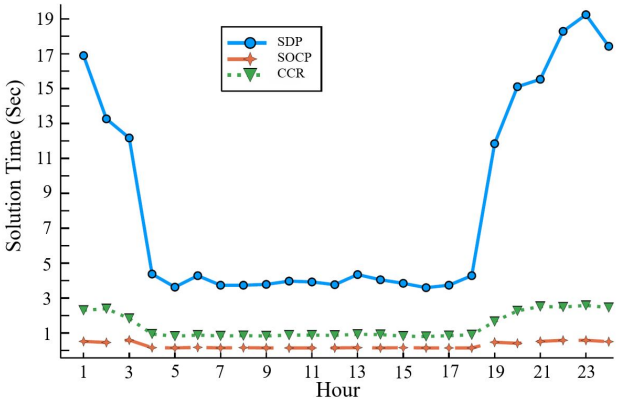

Fig. 5. Comparing the solution time of employing various relaxation methods for 500-bus system

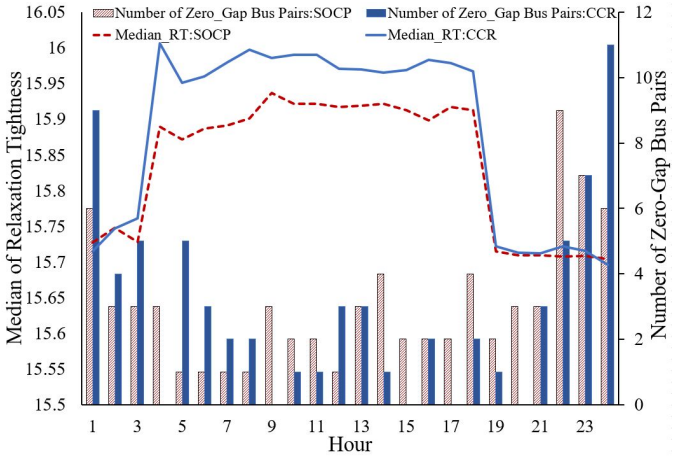

Fig. 6. Comparison between tightness measure and the total number of exact bus-pairs for CCR and SOCP relaxation methods for 500-bus system

C. 793-Bus System

In this section, a modified 793-bus system presented in [35] is considered as a test case. The 793-bus system consists of 912 lines, 210 generators, 143 transformers, and 568 loads. The optimality gap of each method is presented in Table VI, where it is shown that the objective values procured by employing the CCR, sparse SDP, and SOCP relaxation methods are in a close proximity of the objective value procured from employing the non-convex OPF problem which is an upper bound for the optimal solutions. Here, the lower bound for the solutions is $27,479 while the upper bound is $22,480. However, the solution procured by the CCR method is expressing an enhanced tightness compared to the SOCP method. An interesting observation is that the solution rendered by employing CCR is tighter than that of the SOCP relaxation method and is as tight as employing the sparse SDP with a much smaller solution time. Besides, in this case, the

average summation of voltage angle differences of buses over cycles procured by the SOCP relaxation method is 0.53° and it is 32.1% reduced to 0.36° when the CCR relaxation method is employed.

TABLE VI
THE COMPARISON OF OBJECTIVE VALUES AND SOLUTION TIMES OF USING VARIOUS RELAXATION METHODS FOR 793-BUS SYSTEM

	SOCP	SDP	CCR
Objective Value [$]	22,479	22,480	22,480
Solution Time [Sec.]	0.53	30.9	3
Optimality Gap [%]	0.009	0.004	0.004

D. 2000-Bus System

In this section, a modified 2000-bus system presented in [35] is considered as a test case. The 2000-bus system consists of 3206 lines, 544 generators, 1235 transformers, and 1125 loads.

Comparing the number of pairs with zero gap in Table VII illustrates that 51 bus-pairs have zero gap when the CCR method is employed, while this number is 49 when the SOCP relaxation method is employed. The mean, maximum, standard deviation, median, and minimum values of the tightness measures are presented in Table VII. Comparing the mean, maximum, median, and minimum of the finite tightness measures illustrated the superiority of the solution procured by the CCR method compared to the SOCP relaxation method.

TABLE VII
THE COMPARISON OF THE TIGHTNESS MEASURES' STATISTICS WHEN USING VARIOUS RELAXATION METHODS FOR 2000-BUS SYSTEM

Tightness Measure	SOCP	SDP	CCR
Mean	15.83	15.84	15.83
Maximum	18.96	18.42	18.52
Standard Deviation	0.44	0.43	0.43
Median	15.72	15.75	15.74
Minimum	15.05	15.02	15.08
Number of Zero Gap Pairs	49	44	51

As shown in Table VIII, the solution time of employing the CCR method is more than that of the sparse SOCP method. The computational burden of the CCR method is less than the SDP method. The optimality gap of the solution procured by the CCR relaxation method is smaller than the SOCP relaxation method. This verifies the fact that the CCR relaxation method generally renders a tighter solution than the SOCP relaxation method. While the procured CCR solution has a slightly smaller optimality gap than the SDP solution as shown in Table VIII, the mean and median of relaxation tightness measure for the SDP method are higher than that of CCR method as shown in Table VII. Moreover, in this case, the average summation of voltage angle differences of buses over cycles procured by the SOCP relaxation method is 0.1°, and it is 3% reduced to $0.097^\circ$when the CCR method is employed.

TABLE VIII
THE COMPARISON OF THE SOLUTION TIMES USING VARIOUS RELAXATION METHODS FOR 2000-BUS SYSTEM

	SOCP	SDP	CCR
Objective Value [$]	382,357	383,751	383,904
Solution Time [Sec.]	5.37	206.08	139.68
Optimality Gap [%]	0.89	0.52	0.49

V. CONCLUSION

This paper presented a cycle constraint relaxation approach to procure a tight yet computationally efficient solution to the non-convex AC-OPF problem. The non-convex cycle constraint to recover the voltage angle using the SOCP relaxation method is discussed. Then, the second-order moment relaxation matrix is formed to present the lifting term required to present the cycle constraints in the relaxed form. A second-order cone is defined to relate the elements of the procured second-order moment relaxation matrix. The solution procured by the convex relaxation methods is not always feasible for the original non-convex problem. It is illustrated that the proposed approach generally presents a smaller relaxation gap in comparison with SOCP relaxation. The solution time of employing the proposed method is slightly larger than that of the SOCP relaxation method and smaller than that of the sparse SDP relaxation method. This indication is verified in the case study section by comparing these relaxation schemes for four different case studies ranging from small-scale to large-scale systems. The effectiveness of the presented method on enforcing the cycle constraints compared to the SOCP relaxation method is explicitly illustrated. While the focus of this work was not on procuring a feasible solution for the original OPF problem, it is an interesting direction for future studies.

REFERENCES

[1] H. W. Dommel and W. F. Tinney, "Optimal power flow solutions," *IEEE Transactions on power apparatus and systems*, no. 10, pp. 1866–1876, 1968.

[2] S. Frank, I. Steponavice, and S. Rebennack, "Optimal power flow: a bibliographic survey i," *Energy Systems*, vol. 3, no. 3, pp. 221–258, 2012.

[3] S. Frank, I. Steponavice, and S. Rebennack, "Optimal power flow: a bibliographic survey ii," *Energy Systems*, vol. 3, no. 3, pp. 259–289, 2012.

[4] D. I. Sun, B. Ashley, B. Brewer, A. Hughes, and W. F. Tinney, "Optimal power flow by newton approach," *IEEE Transactions on Power Apparatus and systems*, no. 10, pp. 2864–2880, 1984.

[5] W. A. Bukhsh, A. Grothey, K. I. McKinnon, and P. A. Trodden, "Local solutions of the optimal power flow problem," *IEEE Transactions on Power Systems*, vol. 28, no. 4, pp. 4780–4788, 2013.

[6] J. Lavaei and S. H. Low, "Zero duality gap in optimal power flow problem," *IEEE Transactions on Power Systems*, vol. 27, no. 1, pp. 92–107, 2011.

[7] R. A. Jabr, "Optimal power flow using an extended conic quadratic formulation," *IEEE transactions on power systems*, vol. 23, no. 3, pp. 1000–1008, 2008.

[8] C. Coffrin, H. L. Hijazi, and P. Van Hentenryck, "The qc relaxation: A theoretical and computational study on optimal power flow," *IEEE Transactions on Power Systems*, vol. 31, no. 4, pp. 3008–3018, 2015.

[9] B. C. Lesieutre, D. K. Molzahn, A. R. Borden, and C. L. DeMarco, "Examining the limits of the application of semidefinite programming to power flow problems," in *2011 49th annual Allerton conference on communication, control, and computing (Allerton)*. IEEE, 2011, pp. 1492–1499.

[10] B. Kocuk, S. S. Dey, and X. A. Sun, "Inexactness of sdp relaxation and valid inequalities for optimal power flow," *IEEE Transactions on Power Systems*, vol. 31, no. 1, pp. 642–651, 2015.

[11] D. Shchetinin, T. T. De Rubira, and G. Hug, "Efficient bound tightening techniques for convex relaxations of ac optimal power flow," *IEEE Transactions on Power Systems*, vol. 34, no. 5, pp. 3848–3857, 2019.

[12] M. Bynum, A. Castillo, J.-P. Watson, and C. D. Laird, "Strengthened socp relaxations for acopf with mccormick envelopes and bounds tightening," in *Computer Aided Chemical Engineering*. Elsevier, 2018, vol. 44, pp. 1555–1560.

[13] D. K. Molzahn and I. A. Hiskens, "Moment-based relaxation of the optimal power flow problem," in *2014 Power Systems Computation Conference*. IEEE, 2014, pp. 1–7.
[14] J.-B. Lasserre, *Moments, positive polynomials and their applications*. World Scientific, 2010, vol. 1.
[15] M. Fukuda, M. Kojima, K. Murota, and K. Nakata, "Exploiting sparsity in semidefinite programming via matrix completion i: General framework," *SIAM Journal on Optimization*, vol. 11, no. 3, pp. 647–674, 2001.
[16] D. K. Molzahn and I. A. Hiskens, "Sparsity-exploiting moment-based relaxations of the optimal power flow problem," *IEEE Transactions on Power Systems*, vol. 30, no. 6, pp. 3168–3180, 2014.
[17] R. A. Jabr, "Exploiting sparsity in sdp relaxations of the opf problem," *IEEE Transactions on Power Systems*, vol. 27, no. 2, pp. 1138–1139, 2011.
[18] B. Ghaddar, J. Marecek, and M. Mevissen, "Optimal power flow as a polynomial optimization problem," *IEEE Transactions on Power Systems*, vol. 31, no. 1, pp. 539–546, 2015.
[19] D. K. Molzahn and I. A. Hiskens, "Mixed sdp/socp moment relaxations of the optimal power flow problem," in *2015 IEEE Eindhoven PowerTech*. IEEE, 2015, pp. 1–6.
[20] M. Ma, L. Fan, Z. Miao, B. Zeng, and H. Ghassempour, "A sparse convex ac opf solver and convex iteration implementation based on 3-node cycles," *Electric Power Systems Research*, vol. 180, p. 106169, 2020.
[21] S. Bose, S. H. Low, T. Teeraratkul, and B. Hassibi, "Equivalent relaxations of optimal power flow," *IEEE Transactions on Automatic Control*, vol. 60, no. 3, pp. 729–742, 2014.
[22] S. Sojoudi and J. Lavaei, "On the exactness of semidefinite relaxation for nonlinear optimization over graphs: Part i," in *52nd IEEE Conference on Decision and Control*. IEEE, 2013, pp. 1043–1050.
[23] B. Kocuk, S. S. Dey, and X. A. Sun, "Strong socp relaxations for the optimal power flow problem," *Operations Research*, vol. 64, no. 6, pp. 1177–1196, 2016.
[24] Z. Tian and W. Wu, "Recover feasible solutions for socp relaxation of optimal power flow problems in mesh networks," *IET Generation, Transmission & Distribution*, vol. 13, no. 7, pp. 1078–1087, 2019.
[25] R. Madani, S. Sojoudi, and J. Lavaei, "Convex relaxation for optimal power flow problem: Mesh networks," *IEEE Transactions on Power Systems*, vol. 30, no. 1, pp. 199–211, 2014.
[26] H. Hijazi, C. Coffrin, and P. Van Hentenryck, "Polynomial sdp cuts for optimal power flow," in *2016 Power Systems Computation Conference (PSCC)*. IEEE, 2016, pp. 1–7.
[27] R. Louca, P. Seiler, and E. Bitar, "A rank minimization algorithm to enhance semidefinite relaxations of optimal power flow," in *2013 51st Annual Allerton Conference on Communication, Control, and Computing (Allerton)*. IEEE, 2013, pp. 1010–1020.
[28] B. Kocuk, S. S. Dey, and X. A. Sun, "Matrix minor reformulation and socp-based spatial branch-and-cut method for the ac optimal power flow problem," *Mathematical Programming Computation*, vol. 10, no. 4, pp. 557–596, 2018.
[29] R. A. Jabr, "A conic quadratic format for the load flow equations of meshed networks," *IEEE Transactions on Power Systems*, vol. 22, no. 4, pp. 2285–2286, 2007.
[30] C. Coffrin, R. Bent, K. Sundar, Y. Ng, and M. Lubin, "Powermodels. jl: An open-source framework for exploring power flow formulations," in *2018 Power Systems Computation Conference (PSCC)*. IEEE, 2018, pp. 1–8.
[31] S. D. Manshadi, G. Liu, M. E. Khodayar, J. Wang, and R. Dai, "A distributed convex relaxation approach to solve the power flow problem," *IEEE Systems Journal*, 2019.
[32] S. D. Manshadi, G. Liu, M. E. Khodayar, J. Wang, and R. Dai, "A convex relaxation approach for power flow problem," *Journal of Modern Power Systems and Clean Energy*, vol. 7, no. 6, pp. 1399–1410, 2019.
[33] M. ApS, *The MOSEK optimization toolbox for MATLAB manual. Version 9.2.*, 2019.
[34] A. Wächter and L. T. Biegler, "On the implementation of an interior-point filter line-search algorithm for large-scale nonlinear programming," *Mathematical programming*, vol. 106, no. 1, pp. 25–57, 2006.
[35] "Datasets — grid optimization competition," https://gocompetition.energy.gov/challenges/22/datasets, (Accessed on 12/06/2019).

Arash Farokhi Soofi (S'14) received the B.S. and M.S. degrees in electrical power engineering from the Amirkabir University of Technology, Tehran, Iran, in 2015 and 2018, respectively. He is currently pursuing the Ph.D. degree in electrical engineering from the Department of Electrical Engineering, San Diego State University and University of California San Diego, San diego, CA, USA. His current research interests include convex relaxation, bi-level optimization, and power system operation and planning.

Saeed D. Manshadi (M'18) received the B.S. degree from the University of Tehran, Tehran, Iran, in 2012, the M.S. degree from the University at Buffalo, State University of New York, Buffalo, NY, USA, in 2014, and the Ph.D. degree from Southern Methodist University, Dallas, TX, USA, in 2018, all in electrical engineering. He was a Postdoctoral Fellow with the University of California, Riverside, CA, USA. He is currently an Assistant Professor with the Department of Electrical and Computer Engineering, San Diego State University, San Diego, CA, USA. His research interests include smart grids, microgrids, integrating renewable and distributed resources, and power system operation and planning. Dr. Manshadi is an Associate Editor of the IEEE TRANSACTIONS ON VEHICULAR TECHNOLOGY.

Guangyi Liu (SM'12) received the bachelor's, master's, and Ph.D. degrees from the Harbin Institute of Technology, Harbin, China, and China Electric Power Research Institute, Beijing, China, in 1984, 1987, and 1990, respectively. He is a Chief Technology Officer with Global Energy Interconnection Research Institute, North America, San Jose, CA, USA. His research interests include energy management system, distribution management system, electricity market, smart grids, autonomic power system, active distribution network, and application of big data in power system.

Renchang Dai (SM'12) received the Ph.D. degree in electrical engineering from Tsinghua University, Beijing, China, in 2001. He was with Amdocs, GE Global Research Center, Iowa State University, and GE Energy from 2002 to 2017. He is currently with Global Energy Interconnection Research Institute North America, San Jose, CA, USA, as a Manager, Graph Computing and Grid Modernization Group, leading high-performance computing and smart grid research and development.